Author Manuscript

Author Manuscript

Author Manuscript

Author Manuscript

HHS Public Access

Author manuscript

Immunity. Author manuscript; available in PMC 2016 August 18.

Published in final edited form as:

Immunity. 2015 August 18; 43(2): 251–263. doi:10.1016/j.immuni.2015.07.017.

Hydrogen Sulfide Promotes Tet1- and Tet2-mediated *Foxp3* Demethylation to Drive Regulatory T Cell Differentiation and Maintain Immune Homeostasis

Ruili Yang[1,2,3], **Cunye Qu**[3], **Yu Zhou**[4], **Joanne Konkel**[5], **Shihong Shi**[3], **Yi Liu**[6], **Chider Chen**[2,3], **Shiyu Liu**[3], **Dawei Liu**[1], **Yibu Chen**[7], **Ebrahim Zandi**[4], **Wanjun Chen**[5], **Yanheng Zhou**[1,*], and **Songtao Shi**[2,3,*]

[1]Department of Orthodontics, Peking University School & Hospital of Stomatology, #22 Zhongguancun South Avenue, Beijing 100081, China

[2]Department of Anatomy and Cell Biology, University of Pennsylvania, School of Dental Medicine, 240 South 40th Street, Philadelphia, PA, 19104, USA

[3]Center for Craniofacial Molecular Biology, Ostrow School of Dentistry, University of Southern California, 2250 Alcazar Street, CSA 103, Los Angeles, CA 90033, USA

[4]Department of Molecular Microbiology and Immunology, University of Southern California, 2011 Zonal Avenue, Los Angeles, CA 90033, USA

[5]National Institute of Dental and Craniofacial Research, National Institutes of Health, 30 Convent Drive, MSC 4352 Bethesda, MD 20892, USA

[6]Laboratory of Tissue Regeneration and Immunology and Department of Periodontics, Capital Medical University School of Stomatology, #4 Tiantanxili Avenue, Beijing 100050, China

[7]Norris Medical Library, Keck School of Medicine, University of Southern California, 2003 Zonal Ave, Los Angeles, CA 90033, USA

[*]Correspondence: Songtao Shi, DDS, Ph.D., Department of Anatomy and Cell Biology, School of Dental Medicine. University of Pennsylvania, Philadelphia, PA 19104, USA, Tel: 240-793-0641, songtaos@dental.upenn.edu; Dr. Yanheng Zhou, Department of Orthodontics, Peking University School of Stomatology, #22 Zhongguancun South Avenue, Beijing 100081, China, Tel: 86-10-82195381 Fax: 86-10-62173402, yanhengzhou@gmail.com.

Suggested Reviewers:
Dong Chen, cdonglab@hotmail.com, Expert on Tregs
solomon Snyder, ssnyder@jhmi.edu, Expert on H2S

Opposed Reviewers:
Anjana Rao, arao@liai.org, Compete interest
Yujiang Shi, yujiang_shi@hms.harvard.edu, Compete interest
Alexander Rudensky, rudenska@mskcc.org, Conflict of interest
Christophe/Dian Benoist/Mathis, Potential conflict of interest

Publisher's Disclaimer: This is a PDF file of an unedited manuscript that has been accepted for publication. As a service to our customers we are providing this early version of the manuscript. The manuscript will undergo copyediting, typesetting, and review of the resulting proof before it is published in its final citable form. Please note that during the production process errors may be discovered which could affect the content, and all legal disclaimers that apply to the journal pertain.

ACCESSION NUMBER

The Gene Expression Omnibus accession numbers for control and *Cbs*−/− CD4+ T cells microarray data is GSE59241.

AUTHOR CONTRIBUTIONS

S.S., Y.Z., and W.J.C. designed experiments and wrote the manuscript. R. Y. and C.Q. conducted experiments, designed experiments, and organized the manuscript. Y.Z. and E.Z. conducted the Mass analysis. Sh. S., J.K., Y.L., C.C., S.L. and D.L. helped with the mouse management and flow cytometry analysis. Y.C. helped with the microarray analysis.

Author Manuscript Author Manuscript Author Manuscript Author Manuscript

SUMMARY

Regulatory T (Treg) cells are essential for maintenance of immune homeostasis. Here we found that hydrogen sulfide (H_2S) was required for Foxp3$^+$ Treg cell differentiation and function, and that H_2S deficiency led to systemic autoimmune disease. H_2S maintained expression of methylcytosine dioxygenases Tet1 and Tet2 by sulfhydrating nuclear transcription factor Y subunit beta (NFYB) to facilitate its binding to *Tet1* and *Tet2* promoters. Transforming growth factor-β (TGF-β)-activated Smad3 and interleukin-2 (IL-2)-activated Stat5 facilitated Tet1 and Tet2 binding to *Foxp3*. Tet1 and Tet2 catalyzed conversion of 5-methylcytosine (5mC) to 5-hydroxymethylcytosine (5hmC) in *Foxp3* to establish a Treg cell-specific hypomethylation pattern and stable Foxp3 expression. Consequently, *Tet1* and *Tet2* deletion led to *Foxp3* hypermethylation, impaired Treg cell differentiation and function, and autoimmune disease. Thus, H_2S promotes Tet1 and Tet2 expression, which are recruited to *Foxp3* by TGF-β and IL-2 signaling to maintain *Foxp3* demethylation and Treg cell-associated immune homeostasis.

Keywords

Hydrogen Sulfide; regulatory T cells; ten eleven translocation methylcytosine dioxygenases 1 and 2; demethylation; 5-methylcytosine; sulfhydration

INTRODUCTION

Regulatory T (Treg) cells are a distinct lineage of CD4$^+$ T cells that are indispensable in maintaining immune homeostasis and suppressing inflammatory reactions (Vignali et al., 2008). The forkhead-family transcription factor Foxp3 is specifically expressed in Treg cells and plays a crucial role in Treg cell lineage specification and function (Hori et al., 2003). Foxp3 deficiency results in fatal autoimmune disorders in both mice and humans (Shevach, 2000). Treg cell development, differentiation and function are governed by multiple epigenetic regulation mechanisms, such as DNA methylation, histone modifications, and particularly DNA demethylation of *Foxp3* promoter and conserved non-coding DNA sequence (CNS) elements (Kim and Leonard, 2007; Zheng et al., 2010). However, it remains unknown how cell signaling and epigenetic modification are synergistically coordinated to determine Treg cell lineage differentiation and achieve cell identity. DNA methylation has a profound impact on genome stability, gene transcription, and molecular and cellular responses. Recent studies indicate that Ten eleven translocation (Tet) family is capable of converting 5-methylcytosine (5mC) to 5-hydroxymethylcytosine (5hmC) to erase existing methylation marks (Kohli and Zhang, 2013), which serves as an important epigenetics regulation mechanism (Koh et al., 2011; Song et al., 2013). However, the roles of Tet and 5hmC in immune systems, especially in Treg cell development, differentiation and function, are unknown.

Hydrogen sulfide (H_2S), an endogenous gasotransmitter, is capable of regulating various endogenous signaling pathways. In mammals, H_2S is mainly generated by two pyridoxal-5′-phosphate-dependent enzymes, termed cystathionine β-synthase (CBS) and cystathionine γ-lyase (CSE)(Wang, 2002). Impaired H_2S metabolism may be associated with immune disorders, cancer, and hypertension (Peng et al., 2014; Szabo et al., 2013). H_2S may

Author Manuscript Author Manuscript Author Manuscript Author Manuscript

accentuate the inflammatory process in burn injury-induced inflammation and lung injury caused by bacterial sepsis (Li et al., 2005; Zhang et al., 2010). On the other hand, providing H_2S through its donor may be beneficial in the treatment of colitis (Fiorucci et al., 2007), asthma (Zhang et al., 2013), and systemic lupus erythematosus (SLE) (Han et al., 2013). One of the mechanisms by which H_2S regulates inflammation is by sulfhydrating reactive Cys residues in target proteins to increase their catalytic activity (Paul and Snyder, 2012). However, the role of H_2S in inflammation is still under debate and the molecular mechanisms of H_2S in immune regulation remain largely unknown.

In this study, we show that Tet-mediated demethylation of *Foxp3*, in conjunction with signaling modulation, dynamically control Treg cell lineage determination. H_2S deficiency results in reduced Tet1 and Tet2 expression, which leads to hypermethylation of *Foxp3* and, eventually, impairment of Treg cell differentiation and function and immune homeostasis.

RESULTS

Treg Cells Express CBS and CSE and Produce H2S

Since abnormal H_2S metabolism has been linked to defects in immune homeostasis, we revealed that $CD4^+$ T cells produced H_2S in culture supernatant, and which was downregulated by treatment of CBS inhibitor hydroxylamine (HA) or CSE inhibitor D, L-propargylglycine (PAG); conversely, H_2S production was upregulated by treatment with H_2S donor NaHS. Combined treatment with HA and PAG showed similar H_2S decrease as observed in the groups that received HA or PAG individually (Figure 1A). $CD4^+$ T cells from spleen, lymph nodes, and thymus of WT mice expressed both mRNA and protein of CBS and CSE (Figure 1B–D). Expression of *Cbs* and *Cse* in Treg cells were elevated compared to other $CD4^+$ T cell subsets (Figure 1E). Treg cells also produced H_2S in the culture supernatant, which was regulated by H_2S inhibitor HA and PAG or H_2S donor (Figure 1F).

H2S-deficient Mice Show Treg Cell Deficiency and Autoimmune Disease

Treatment with the H_2S inhibitors HA and PAG led to reduced Treg cell numbers in mouse spleen and lymph nodes with a similar reduction observed with combined or single HA and PAG treatment (Figure 1G, 1H and Figure S1A). Moreover, HA, PAG or HA and PAG treatment reduced Treg cell differentiation *in vitro* when cultured with different doses of TGF-β1 (Figure S1B) (Chen et al., 2003).

To further examine whether H_2S serves as a physiologic gasotransmitter for regulating T cells, we analyzed Treg cell differentiation and function in H_2S-deficient ($Cbs^{-/-}$) mice (Figure S2A, S2B) (Watanabe et al., 1995). $Cbs^{-/-}$ mouse serum showed decreased concentrations of H_2S compared to control ones (Figure S2C). $CD4^+$ T cells from $Cbs^{-/-}$ mice also produced less H_2S when cultured *in vitro* (Figure S2D). Consistent with H_2S inhibitor HA and PAG treatment, the proportion of $Foxp3^+$ Treg cells were reduced in the spleen and lymph nodes of $Cbs^{-/-}$ mice compared to control littermates (Figure 2A). The total number of Treg cells was also diminished in $Cbs^{-/-}$ mice (Figure 2B). $Cbs^{-/-}$ T cells showed compromised *in vitro* Treg cell differentiation when cultured with different doses of

Author Manuscript Author Manuscript Author Manuscript Author Manuscript

TGF-β1 (Figure 2C). Moreover, $CD4^+Foxp3^+$ Treg cells from *Cbs*$^{-/-}$ mice exhibited a reduced capacity to suppress $CD4^+CD25^-$ T cells, as assessed by an *in vitro* coculture assay (Figure 2D). To validate these findings we generated *Cbs*$^{-/-}$ *Foxp3*^{GFP} mice by crossing *Cbs*$^{+/-}$ mice with *Foxp3*^{GFP} mice. As expected, *Cbs*$^{-/-}$*Foxp3*^{GFP} mice showed reduced numbers of GFP-labeled Treg cells compared to *Foxp3*^{GFP} mice (Figure 2E). Moreover, Foxp3 expression was reduced in *Cbs*$^{-/-}$ Treg cells, as indicated by reduced mean fluorescence intensity (MFI) (Figure 2F). We observed that autoreactive antibodies, including total immunoglobulin M (IgM) (Figure 2G), anti-nuclear antibody (ANA) (Figure 2H), and anti-double strand DNA (dsDNA) IgG and IgM antibodies (Figure 2I), were more abundant in serum from *Cbs*$^{-/-}$ mice compared to control ones. *Cbs*$^{-/-}$ mice were born in expected Mendelian ratios and appeared grossly normal at the newborn stage. However, they started to lose body weight at 4 weeks of age, along with a high incidence of death may be owe to inflammation of multiple organs, including the colon, lung and liver (Figure 2J–2L and Figure S2E). We found a consistent decrease in the proportion of Treg cells in the lung, gut and liver of *Cbs*$^{-/-}$ mice (Figure S2F). Analysis of peripheral $CD4^+$ T cells obtained from peripheral lymphoid organs showed that effector T cell numbers were elevated in *Cbs*$^{-/-}$ mice (Figure S2G). *Cbs*$^{-/-}$ mice showed increased $CD4^+IL\text{-}17^+$ and $CD4^+IFN\text{-}\gamma^+$ cells in the peripheral lymphoid organs compared to control ones, though there was no difference in the number of $IL\text{-}4^+$ cells (Figure S2H, S2I), while $CD4^+$ cell distributions in the peripheral lymphoid organs of *Cbs*$^{-/-}$ mice were similar to the control group (Figure S2J). To verify the role of H_2S in Treg cell development, we generated mixed bone marrow chimeras by injecting C57BL/6 ($CD45.1^+$) control bone marrow with *Cbs*$^{-/-}$ ($CD45.2^+$) bone marrow into sublethally irradiated *Rag1*$^{-/-}$ recipient mice. We showed that the recipient mice had a reduced proportion of $CD4^+Foxp3^+$ Treg cells originating from *Cbs*$^{-/-}$ bone marrow compared to those originating from control mice (Figure S2K), indicating that endogenous H_2S production plays an essential role in Treg cell generation. To examine whether inflammation in *Cbs*$^{-/-}$ mice is an autoimmune response, we transferred $CD4^+$ naïve T cells, derived from control and *Cbs*$^{-/-}$ mice, into *Rag1*$^{-/-}$ mice and found that *Cbs*$^{-/-}$ T cells elicited a more severe immune response, as indicated by signs of severe colitis and more body weight loss compared to the control group (Figure S2L–S2O). When transferred into *Rag1*$^{-/-}$ mice together with *Cbs*$^{-/-}$ Treg cells, failed to prevent development of colitis, confirming the compromised suppressive capacity of *Cbs*$^{-/-}$ Treg cells (Figure S2L–S2O). These data suggest that H_2S deficiency is associated with the development of autoimmune disease.

H_2S Promotes Immune Homeostasis *via* Regulating Treg Cells

To further determine whether Treg cell deficiency accounted for autoimmunity in *Cbs*$^{-/-}$ mice, we transferred WT Treg cells into *Cbs*$^{-/-}$ mice and found that Treg cell transfer increased body weight of *Cbs*$^{-/-}$ mice (Figure 3A). The elevated levels of autoreactive antibodies including anti-IgM, ANA, anti-ds DNA antibodies in *Cbs*$^{-/-}$ mice were partially blocked by Treg cell transfer (Figure 3B–3D). Moreover, survival analysis indicated that WT Treg cell transfer (n=6) extended life span of *Cbs*$^{-/-}$ mice (n=10) (Figure 3E). The elevated inflammatory cells infiltration observed in the colon, liver and lung of *Cbs*$^{-/-}$ mice also rescued by Treg cell infusion (Figure 3F). These results indicate that Treg cell deficiency at least partially accounts for the autoimmunity developed in *Cbs*$^{-/-}$ mice.

Author Manuscript Author Manuscript Author Manuscript Author Manuscript

Microarray and gene set enrichment analysis (GSEA) of $CD4^+$ T cells from *Cbs*$^{-/-}$ and control mice (Figure S3A, S3B) showed reduced expression of *Foxp3*-related genes in *Cbs*$^{-/-}$ mice (Figure S3B). The downregulated expression of *Foxp3*-related genes in $CD4^+$ T cells using qPCR validated the microarray data. Moreover, the expression of *Foxp3*-related genes was downregulated in *Cbs*$^{-/-}$ Treg cells (Zheng et al., 2007) (Figure S3C), suggesting that H_2S deficiency may affect expression of Foxp3 and its downstream genes.

We next examined whether H_2S donor treatment could rescue Treg cell numbers and autoimmunity phenotypes in *Cbs*$^{-/-}$ mice and showed that injection of H_2S donor GYY4137 (Figure S3D) resulted in increased serum H_2S concentrations and body weight (Figure 3A and Figure S3E). The elevated autoreactive antibodies in *Cbs*$^{-/-}$ mice were partially decreased after H_2S donor treatment along with an extended life span and decreased inflammatory cells infiltration in the colon, liver and lung of *Cbs*$^{-/-}$ mice (Figure 3B–3F). The frequency of Treg cells was elevated by GYY4137 treatment in *Cbs*$^{-/-}$ mice (Figure 3G). There was no obvious change in control mice when receiving H_2S donor treatment (Figure 3A–3G). These results indicate that elevating H_2S levels are capable of restoring immune homeostasis and Treg cell numbers in *Cbs*$^{-/-}$ mice.

H_2S deficiency-induced homocysteine (Hcy) accumulation may contribute to disease phenotypes in patients (Kelly et al., 2003). As Hcy concentrations are higher in *Cbs*$^{-/-}$ mouse serum than in control mouse serum (Liu et al., 2014), we treated mice with Hcy and found that Hcy failed to affect Treg cell numbers (Figure S3F). These data indicate that H_2S, but not homocysteine, regulates Treg cells.

Analysis of AnnexinV, 7AAD and Ki67 showed rate of apoptosis and proliferation in $CD4^+Foxp3^+$ Treg cells from *Cbs*$^{-/-}$ and control mice were similar (Figure S3G, S3H).

H_2S Targets Tet1 and Tet2 to Regulate Hydroxylation of 5mC

Since *Cbs*$^{-/-}$ Treg cells had decreased expression of Foxp3 and its target genes, including CD25, GITR and CTLA-4 (Figure S4A), we used qPCR and Western blot analysis to confirm that *Cbs*$^{-/-}$ Treg cells had decreased expression of Foxp3 (Figure 4A and Figure S4B). We next examined why H_2S-deficent Treg cells express reduced amount of Foxp3 and found *Cbs*$^{-/-}$ T cells expressed similar levels of phosphorylated Smad3 and Stat5 to those of control cells treated by TGF-β1 or IL-2 *in vitro* (Figure S4C, S4D), which indicate that H_2S regulate Foxp3 expression in Treg cells may not *via* different response to TGF-β1 and IL-2 signaling. Foxp3 expression is controlled by its promoter region and intragenic enhancer elements CNS1-3 (Zheng et al., 2010). CpG motifs in CNS2 are demethylated in Treg cells, which are known to be required for stable Foxp3 expression (Floess et al., 2007). Thus, we examined the methylation status of the promoter and CNS2 in *Foxp3* locus. $CD4^+CD25^+$ Treg cells and $CD4^+CD25^-$ T conventional cells (Tconv) were isolated and their methylation status was analyzed (Kim and Leonard, 2007). In comparison to Treg cells, Tconv cells showed high amounts of methylation in the promoter and CNS2 of *Foxp3* locus. However, Treg cells from *Cbs*$^{-/-}$ mice displayed elevated methylation in the promoter and CNS2 of *Foxp3* locus compared to Treg cells from control mice (Figure 4B), suggesting that H_2S plays a functional role in DNA demethylation of *Foxp3* locus. Genomic DNA is mainly methylated by DNA methyltransferases (Dnmt family members), whereas it can be

Author Manuscript Author Manuscript Author Manuscript Author Manuscript

demethylated in multiple ways, including Tet-mediated 5mC hydroxylation (Kohli and Zhang, 2013). We found that *Dnmt* expression was not altered in *Cbs*$^{-/-}$ CD4^{+} T cells (Figure S4E). The Tet family contributes to DNA demethylation by converting 5mC to 5hmC, and has recently been implicated in epigenetic regulation of cell reprogramming and differentiation (Tahiliani et al., 2009). Using western blot and qPCR analysis, we found H_2S deficiency led to downregulation of Tet1 and Tet2, but not Tet3, in CD4^{+} T cells (Figure 4C, 4D and Figure S4F). H_2S inhibitors HA or PAG treatment resulted in downregulation of Tet1 and Tet2 in CD4^{+} T cells (Figure S4G, S4H), whereas treatment with H_2S donor NaHS rescued Tet1 and Tet2 expression in *Cbs*$^{-/-}$ CD4^{+} T cells (Figure 4E and Figure S4I). These data suggest that H_2S is required for maintenance of Tet1 and Tet2 expression.

Tet-mediated active DNA demethylation within *Foxp3* may be involved in Treg cell development (Toker et al., 2013). We next investigated whether H_2S regulated 5hmC enrichment within *Foxp3* locus and found that 5hmC enrichment was decreased within *Foxp3* promoter, CNS2 and CNS3 in *Cbs*$^{-/-}$ Treg cells compared to the control ones, as assessed by hMeDIP-qPCR analysis (Figure 4F). In contrast, 5mC enrichment was elevated within *Foxp3* promoter, CNS2, and CNS3 in *Cbs*$^{-/-}$ Treg cells (Figure 4G). These data suggest that H_2S may regulate 5hmC enrichment in *Foxp3* locus. We next assessed whether H_2S modified the epigenetic landscape by affecting 5hmC levels in the genome. Dot blot assays and immunofluorescence analysis showed that global 5hmC levels were decreased in *Cbs*$^{-/-}$ CD4^{+} T cells (Figure 4H, 4I). More importantly, H_2S donor NaHS treatment rescued global 5hmC levels in a time-dependent manner (Figure 4J). Since *Foxp3* promoter and CNS element epigenetic marks play important roles in determining Treg cell identity, we examined whether H_2S was required to stabilize the expression of Foxp3. We found that *Cbs*$^{-/-}$ Treg cells had reduced Foxp3 expression compared to the corresponding *Foxp3*^{GFP} Treg cells after 3 days of culture *in vitro* (Figure S4J). Moreover, *Cbs*$^{-/-}$ Treg cells were much easier to differentiate into Th1 and Th17 cells, but not into Th2 cells, when cultured *in vitro* (Figure S4K–S4M). Taken together, these data suggest that H_2S-mediated enrichment of 5hmC in *Foxp3* locus may contribute to Treg cell differentiation, function and stability.

H_2S Regulates Tet1 and Tet2 Expression *via* Sulfhydration of NFYB

Tet enzyme expression is under tight transcriptional regulation. For instance, OCT4 and C/EBPα directly associate with *Tet and Tet2* promoters and regulatory elements to regulate their expression in pluripotent stem cells and myeloid lineage cells (Kallin et al., 2012; Koh et al., 2011). Since analysis of *Tet1 and Tet2* promoters (Transfec, Biobase) showed conserved CCAAT binding motif for NFY, which is a well-characterized heterotrimeric transcriptional activator (NFYA, NFYB, and NFYC), we verified that NFYB bound to the promoters of *Tet1 and Tet2* by ChIP-qPCR analysis. This binding was decreased in *Cbs*$^{-/-}$ CD4^{+}T cells. When treated with H_2S donor, but not H_2S substrate L-cysteine, NFYB binding to *Tet1* and *Tet2* promoters were restored in *Cbs*$^{-/-}$ T cells (Figure 5A), indicating H_2S may facilitate NFYB binding to *Tet1* and *Tet2* promoters. Knockdown of *Nfyb* by siRNA led to decreased expression of Tet1 and Tet2 as well as partially suppressed H_2S-induced upregulation of Tet1 and Tet2 in CD4^{+} T cells (Figure 5B, 5C and Figure S5A). However, we found that *Cbs*$^{-/-}$ and control cells expressed similar amounts of NFYB (Figure 5D).

Author Manuscript Author Manuscript Author Manuscript Author Manuscript

Ubiquitination at Lys138 is important for NFYB transcriptional activation (Nardini et al., 2013), implying that protein modification may regulate NFYB activity. H_2S mediates signal response predominantly by sulfhydrating cysteines of target proteins such as GAPDH and actin, leading to augmentation of GAPDH catalytic activity and actin polymerization (Mustafa et al., 2009). Sulfhydration (SHY) is a physiological process in which H_2S attaches an additional sulfur to the thiol (-SH) group of a cysteine, yielding a hydropersulfide (-SSH) (Sen et al., 2012). We employed Alexa Fluor 488-conjugated C5 maleimide (green maleimide), which interacts selectively with sulfhydryl groups of cysteines, to label both sulfhydrated and unsulfhydrated cysteines. Dithiothreitol (DTT) treatment was used to selectively cleave disulfide bonds and detach the green signal from sulfhydrated protein only, resulting in decreased fluorescence (Figure 5E). We used the green maleimide to detect overall protein sulfhydration in T cell lysates. In control T cells, we detected green bands representing proteins with SH and SSH in the presence of L-cysteine, and observed a 50% reduction of the green signal after DTT treatment. Green signals were also detected in *Cbs*$^{-/-}$ T cells; however, DTT treatment failed to reduce the green signals (Figure S5B). DTT treatment abolished the green NFYB signal in the presence of L-cysteine in control T cells, indicating sulfhydration of NFYB. In contrast, in *Cbs*$^{-/-}$ T cells, DTT did not affect the green NFYB signal, indicating absence of NFYB sulfhydration in *Cbs*$^{-/-}$ T cells (Figure 5F). Treatment with H_2S donor NaHS improved sulfhydration of NFYB in control T cells, and also restored sulfhydration of NFYB in *Cbs*$^{-/-}$ T cells (Figure 5G). We next employed liquid chromatography-mass spectrometric analysis (LC-MS) to identify the cysteine residue responsible for sulfhydration of NFYB under H_2S donor treatment (Liu et al., 2014). The mass shift suggested that the cysteine residues (C) were sulfhydrated at the C105 site of NFYB after H_2S donor treatment (Figure 5H and Figure S5C). To verify the effect of sulfhydration on NFYB binding to *Tet1* and *Tet2* activity, we used diamide (DM), which is capable of reducing the number of sulfhydryls and thereby reducing protein sulfhydration (Kosower et al., 1969), to pretreat *Cbs*$^{-/-}$ T cells. ChIP-qPCR results showed that DM treatment blocked H_2S donor-induced rescue of NFYB binding to *Tet1* and *Tet2* promoters (Figure 5I). To further confirm that sulfyhydration of NFYB cysteine residues played a critical role in H_2S-mediated Tet1 and Tet2 expression, we generated *Nfyb* C105 mutation constructs (*Nfyb* C105A) and overexpressed *Nfyb* and *Nfyb* C105A in CD4$^+$ T cells (Figure 5J and Figure S5D). Overexpression of *Nfyb* elevated Tet1 and Tet2 expression, especially under H_2S donor treatment (Figure 5K, 5L). However, overexpression of *Nfyb* C105A failed to upregulate expression of Tet1 and Tet2 either with or without H_2S donor treatment (Figure 5K, 5L), indicating that H_2S-regulated Tet1 and Tet2 expression in CD4$^+$ T cells depends at least partially on the sulfhydration of NFYB C105. These results suggest that H_2S-mediated sulfhydration of NFYB is important for NFY complex binding to *Tet1* and *Tet2* promoters to regulate their expression.

Loss of Tet1 and Tet2 Impair Treg Cell Differentiation and Function

In order to verify the role of Tet1 and Tet2 in immune homeostasis and Treg cell differentiation and function, we generated *Tet1*$^{-/-}$; *Cd4*^{Cre}; *Tet2*$^{fl/fl}$ double knockout (*Tet* DKO) mice (Figure S6A) and found that they developed inflammation in multiple organs, including the colon, lung and liver (Figure 6A), along with infiltration of abundant CD3-positive cells (Figure S6B), decreased body weight (Figure S6C), and several elevated

Author Manuscript Author Manuscript Author Manuscript Author Manuscript

autoantibodies, including anti-dsDNA IgG (Figure 6B) and IgM (Figure 6C) antibodies, and anti-ANA (Figure 6D) in the peripheral blood. Treg cell frequencies in *Tet* DKO mice were significantly decreased in spleen and lymph nodes compared to the control group (Figure 6E). In addition, total numbers of Treg cells were decreased in *Tet* DKO mice (Figure 6F). *Tet* DKO Treg cells also showed reduced Foxp3 expression (Figure 6G–6I). These results indicate that *Tet1* and *Tet2* depletion lead to reduction of Treg cell frequency and Foxp3 expression. The proportion of Treg cells were also consistently decreased in the lung and liver in *Tet* DKO mice (Figure S6D). Moreover, Treg cells from *Tet* DKO mice showed reduced capacity to suppress $CD4^+CD25^-$ cells, as assessed by *in vitro* coculture assay (Figure 6J). The experimental data imply that Tet1 and Tet2 are required for maintenance of immune homeostasis and Treg cell differentiation and function.

Next, we generated mixed bone marrow chimeras to confirm the intrinsic role of Tet1 and Tet2 in $CD4^+Foxp3^+$ Treg cell generation. We injected C57BL/6 ($CD45.1^+$) bone marrow with *Tet* DKO ($CD45.2^+$) bone marrow into sublethally irradiated WT recipient mice. We revealed that the recipient mice had a reduced proportion and numbers of $CD4^+Foxp3^+$ Treg cells originating from *Tet* DKO mouse bone marrow compared to those originating from the control ones (Figure 6K–6L), indicating that Tet1 and Tet2 intrinsically regulate Treg cell differentiation. T cells from *Tet* DKO mice displayed slightly decreased Treg cell differentiation in the presence of TGF-β and IL-2 (Figure S6E). Furthermore, *Tet1* and *Tet2* depletion resulted in reduced global 5hmC levels in $CD4^+$ T cells (Figure S6F) and 5hmC enrichment within *Foxp3* promoter, as well as CNS2 and CNS3 in Treg cells, as assessed by hMeDIP-qPCR (Figure 6M). The enrichment of 5mC within *Foxp3* promoter and CNS2 were elevated in *Tet* DKO Treg cells, as assessed by MeDIP-qPCR (Figure 6N). We found that Tconv cells from both *Tet* DKO and control mice were high methylated in the *Foxp3* promoter and CNS2 region, while *Tet1* and *Tet2* depletion resulted in reduced DNA demethylation in Treg cells compared to controls (Figure 6O and Figure S6G). Similar to $Cbs^{-/-}$ Treg cells, *Tet1* and *Tet2* depleted Treg cells expressed reduced amounts of Foxp3 after 3 days *in vitro* culture. *Tet* DKO Treg cells were much easier to differentiate into Th1 and Th17 cells, but not into Th2 cells, when cultured *in vitro* (Figure S6H–S6K). To verify the role of Tet1 and Tet2 in Treg cell differentiation and function, we showed that WT control Treg cells adaptively transferred into *Tet* DKO mice were capable of ameliorating systemic inflammatory phenotypes, as shown by reduction of the elevated levels of autoreactive antibodies, improvement of histopathological alteration in the colon, liver and lung, elevation of the body weight and extension of mouse life span (Figure S6L–S6Q). We next generated $Tet1^{-/-}$;$Foxp3^{Cre}$;$Tet2^{fl/fl}$ double knockout (*Tet* KO) mice and found these mice developed similar inflammation phenotypes to those observed in *Tet* DKO mice, such as multiple organs inflammation, elevated autoreactive antibodies, decreased body weight and higher incidence of death (Figure S6L–S6Q). In addition, *Tet* KO mice showed decreased Treg cell frequency and Foxp3 expression in Treg cells (*Foxp3* demethylation and Treg cell differentiation and function.

Smad3 and Stat5 Recruit Tet Proteins to *Foxp3* Locus

Previous studies showed that 5hmC colocalized with Tet1 at high and intermediate GpG-content sequences (Xu et al., 2011). To investigate whether *Foxp3* is a direct target of Tet1

Author Manuscript Author Manuscript Author Manuscript Author Manuscript

and Tet2, we showed that Tet1 and Tet2 bound to *Foxp3* promoter and CNS1-3 regions with different enrichment levels, which were decreased in *Cbs*$^{-/-}$ Treg cells compared to the control group (Figure 7A). Since TGF-β and IL-2 play indispensable role in Treg cell development, differentiation and cell identity (Chen et al., 2003; Feng et al., 2014; Konkel et al., 2014; Li et al., 2014), we examined whether TGF-β and IL-2 signaling regulate Tet1 and Tet2 expression and found that TGF-β and IL-2 treatment failed to affect expression of Tet1 and Tet2 or global 5hmC levels in T cells (Figure 7B, 7C). Since Tet1 and Tet2 can interact with other molecules, such as NANOG, to synergistically regulate cell signaling for reprogramming (Costa et al., 2013), we assessed whether TGF-β and IL-2 treatment regulated Tet1 and Tet2 interaction with protein complexes in T cells. We used LC-MS analysis to show that Smad3 and Stat5a interacted with both Tet1 and Tet2 in CD4$^+$ T cells and Treg cells (Figure S7A–S7C, Table S1). Next, we performed immunoprecipitation to show that Tet1 and Tet2 co-immunoprecipitated with Smad3 and Stat5 to a higher degree in Treg cells compared to CD4$^+$ T cells. TGF-β and IL-2 treatment enhanced co-immunoprecipitation of Smad3 and Stat5 with Tet1 and Tet2 in T cells while TGF-β and IL-2 neutralizing antibody attenuated the co-immunoprecipitation of Smad3 and Stat5 with Tet1 and Tet2 in Treg cells (Figure 7D). Stat5 binds to *Foxp3* promoter and CNS2 region, serving as a key regulator to open CNS2 region to maintain Treg cell identity, and CNS1 is a TGF-β-sensitive element that contains binding sites for NFAT and SMADs (Feng et al., 2014; Ogawa et al., 2014). Treg cells showed higher enrichment of Tet1 and Tet2 on *Foxp3* promoter and CNS2 compared to CD4$^+$ T cells (Figure 7E, 7F). To determine the role of TGF-β and IL-2 in regulating Tet1 and Tet2 binding to *Foxp3* locus, we showed that TGF-β and IL-2 treatment elevated Tet1 and Tet2 binding to *Foxp3* promoter, CNS1 and CNS2, but not CNS3 in CD4$^+$ T cells, while TGF-β and IL-2 neutralizing antibody treatment abolished Tet1 and Tet2 binding to *Foxp3* locus in Treg cells (Figure 7E, 7F). To verify the roles of protein interaction and recruitment in *Foxp3* demethylation, CD4$^+$CD25$^-$Foxp3^{GFP-} T cells from control or *Tet* DKO mice were transferred to *Rag1*$^{-/-}$ mice and a fraction of CD4$^+$Foxp3^{GFP+} cells were generated. These cells showed progressive demethylation of *Foxp3* promoter and CNS2 regions (Figure 7G). Moreover, CD4$^+$Foxp3^{GFP+} from the *Tet* DKO T cell transfer group showed reduced demethylation compared to the control group at *Foxp3* promoter and CNS2 region. Smad3 and Stat5 knockdown decreased demethylation of *Foxp3* promoter and CNS2 compared to the scramble control group (Figure 7G and Figure S7D). Taken together, these findings indicate that TGF-β and IL-2 activated Smad3 and Stat5, recruiting Tet1 and Tet2 binding to *Foxp3* locus to regulate *Foxp3* demethyaltion and Treg cell differentiation and function.

H_2S Donor Treatment Rescues Treg Cell Deficiency in *Cbs*$^{-/-}$ Mice in a Tet-Dependent Manner

We next examined whether rescue of Treg cell deficiency by H_2S donor depended on Tet1 and Tet2 and found that H_2S donor NaHS treatment failed to rescue Treg cell numbers decrease in *Tet* DKO mice (Figure 7H). When we infused *Tet1* and *Tet2* overexpressed CD4$^+$CD25$^-$Foxp3^{GFP-} T cells to *Rag1*$^{-/-}$ mice, the *Tet1* and *Tet2* overexpression group had an increased numbers of CD4$^+$Foxp3$^+$ Treg cells relative to the control group (Figure 7I and Figure S7E). We further analyzed Tet1 and Tet2 expression in CD4$^+$ T cells from H_2S donor GYY4137 injection mice and found that Tet1 and Tet2 was elevated after GYY4137

Author Manuscript Author Manuscript Author Manuscript Author Manuscript

treatment in *Cbs*$^{-/-}$ mice (Figure 7J and Figure S7F). HMeDIP-qPCR analysis showed that GYY4137 injection elevated 5hmC enrichment within *Foxp3* locus in Treg cells from *Cbs*$^{-/-}$ mice (Figure 7K). These data indicate that the role of H_2S in regulating Treg cell differentiation and function depends on Tet-mediated demethyaltion.

DISCUSSION

We showed that reduced levels of H_2S were responsible for the impairment of CD4$^+$Foxp3$^+$ Treg cell differentiation and function and systemic autoimmune disease observed in mice. Administration of H_2S donor could rescue Treg cell deficient and systemic autoimmune phenotypes in *Cbs*$^{-/-}$ mice and WT Treg cell infusion could also partially rescue autoimmunity in *Cbs*$^{-/-}$ mice, suggesting that H_2S is indispensable for Treg cell-associated immune homeostasis.

Epigenetic modifications, especially DNA methylation, play an important role in immune system and Foxp3$^+$ Treg cell differentiation and lineage stabilization (Ichiyama et al., 2015; Kim and Leonard, 2007; Tsagaratou et al., 2014). Tet expression is important for *Foxp3* demethylation establish and maintain in the thymus and peripheral Treg cells and may play an essential role in Treg cell development, differentiation and function as well as the maintenance of immune homeostasis (Nair and Oh, 2014; Toker et al., 2013; Wang et al., 2013). Our results showed that deletion of *Tet1* and *Tet2* resulted in systemic autoimmune disease due to a substantial reduction and impairment of Treg cell differentiation and function. *Tet*-deleted Treg cells showed substantially reduced enrichment of 5hmC within *Foxp3* promoter and CNS elements, which may be responsible for Treg cell deficiency. However, whether Tet family members regulate other types of cells in the immune system still needs further investigation. DNA methylation and demethylation are regulated by multiple factors (Wu and Zhang, 2014). *Cbs*$^{-/-}$ and *Tet* DKO Treg cells showed hypermethylation at *Foxp3* promoter and CNS2, with variable methylation ratio per cell. Based on Foxp3 expression, Treg cells can be classified into Foxp3^{low}, Fopx3^{med} and Foxp3^{high} subsets. Among these, the Foxp3^{low} subsets were substantially reduced in *Foxp3* CNS2 knockout mice (Li et al., 2014), implying that different Treg cell subsets may be regulated differently based on *Foxp3* expression or methylation.

The H_2S-medidated protein sulfhydration may affect its regulatory effects on inflammatory processes and vasorelaxation (Paul and Snyder, 2012). H_2S could sulfhydrate NFYB to control its binding activity to *Tet1* and *Tet2* promoters, and thus regulated Tet1 and Tet2 expression in Treg cells. This may illustrate the underlying mechanism of how sulfhydration was involved in inflammatory processes. Strikingly, H_2S-mediated sulfhydration may represent a new protein modification approach to regulate NFYB function, similar to the ubiquitination of NFYB at Lys138 to regulate transcriptional activation (Nardini et al., 2013). H_2S affected sulfhydration of NFYB to control NFYB complex binding to the promoters of *Tet1 and Tet2,* forming a H_2S-NFYB-Tet axis, thus regulating Treg cell differentiation and function. Tet-mediated 5mC hydroxylation has been detected in a broad range of cell types and extensively studied in embryonic stem cells (ESCs), brain cells and neurons (Kriaucionis and Heintz, 2009; Tahiliani et al., 2009). H_2S exerts multifaceted and important effects on the central nervous system and NFY is required for maintenance of

Author Manuscript Author Manuscript Author Manuscript Author Manuscript

ESC properties and neuronal cell functions(Grskovic et al., 2007; Yamanaka et al., 2014). These pieces of evidence suggest that the H_2S-NFYB-Tet regulation cascade may be applicable to other cell types.

Tet1 binds to target genes either to regulate the metabolism of 5mC at CpG-rich sequences by converting it to 5hmC, or to regulate transcription. For example, Tet1 is involved in transcriptional repression through its interaction with the SIN3A complex (Williams et al., 2011) and establishes cell pluripotency through its interaction with NANOG (Costa et al., 2013). We showed that phosphorylated Smad3 and Stat5, upon stimulation by TGF-β and IL-2, facilitated Tet1 and Tet2 binding to *Foxp3* locus. This was achieved *via* the formation of a protein complex, leading to the enrichment of 5hmC to promote Foxp3 expression and Treg cell differentiation and function. Stable Treg cell lineage establishment requires concurrent expression of the transcription factor Foxp3 and establishment of Treg cell-specific hypomethylation pattern (Ohkura et al., 2012). Our study indicates that Treg cell lineage determination and maintenance require synergistic regulation by signaling pathway and epigenetic modification, in which Tet1 and Tet2 are required for the dynamic process that establishes and maintains hypomethylation of *Foxp3*.

In conclusion, physiological levels of H_2S are required to maintain immune homeostasis by regulating Tet expression in T cells. Treg cell lineage determination and maintenance require synergistic regulation by signaling pathway and epigenetic modification.

EXPERIMENTAL PROCEDURES

Mice

C57BL/6 (JAX #000664), B6.SJL-Ptprc^{a} (JAX #002014, CD45.1^{+}), B6.129S7-*Rag1*^{tm1Mom}/J (JAX #002216, *Rag1*$^{-/-}$), B6.129P2-*Cbs*^{tm1Unc}/J (JAX #002461, *Cbs*$^{+/-}$), B6.Cg-Foxp3^{tm2Tch}/J (JAX #006772, *Foxp3*^{GFP}), B6.129S4-*Tet1*$^{tm1.1Jae}$/J (JAX #017358, *Tet1*$^{+/-}$), B6.129S-*Tet2*$^{tm1.1Iaai}$/J (JAX #017573, *Tet2*$^{fl/fl}$), and Tg (Cd4-cre)1Cwi/BfluJ (JAX #017336, *Cd4*^{Cre}). To generate *Cbs*$^{-/-}$; *Foxp3*^{GFP} mice, we mated *Cbs*$^{+/-}$ mice with *Cbs*$^{+/-}$; *Foxp3*^{GFP} mice. To generate *Tet1*$^{-/-}$;*Cd4*^{Cre};*Tet2*$^{fl/fl}$ mice, we mated *Tet1*$^{+/-}$;*Cd4*^{Cre};*Tet2*$^{fl/+}$ mice with *Tet1*$^{+/-}$;*Tet2*$^{fl/fl}$ mice. To generate *Tet1*$^{-/-}$/*Cd4*^{Cre}; *Tet2*$^{fl/fl}$; *Foxp3*^{GFP} mice, we mated *Tet1*$^{+/-}$;*Cd4*^{Cre};*Tet2*$^{fl/+}$;*Foxp3*^{GFP} mice with *Tet1*$^{+/-}$;*Tet2*$^{fl/fl}$ mice. All animal experiments were performed under institutionally approved protocols for the use of animal research at the University of Southern California (USC#11141, 11953 and 11327).

Adoptive Transfer Colitis

Rag1$^{-/-}$ mice were injected intravenously with 4×10^5 FACS-sorted naive CD4^{+}CD25^{-}CD45RB^{high} cells from control or *Cbs*$^{-/-}$ mice, without or with control or *Cbs*$^{-/-}$ 2×10^5 Treg cells. After T-cell reconstitution, mice were monitored weekly and samples were harvested six weeks later for further investigation.

Author Manuscript Author Manuscript Author Manuscript Author Manuscript

Generation of Mixed Bone Marrow Chimeric Mice

Bone marrow cells were isolated from femurs and tibias of donor animals (*Tet1*$^{-/-}$;*Cd4*^{Cre};*Tet2*$^{fl/fl}$ CD45.2 or *Cbs*$^{-/-}$ CD45.2 and WT CD45.1). C57BL/6 WT mice received sublethal irradiation (10 Gy). At 6 hour post-irradiation, *Tet1*$^{-/-}$;*Cd4*^{Cre};*Tet2*$^{fl/fl}$ CD45.2 cells (1×10^6) or *Cbs*$^{-/-}$ CD45.2 cells (1×10^6) and WT CD45.1 cells (1×10^6) were infused into irradiated C57BL/6 WT mice. Eight weeks later, mice were sacrificed and analyzed using flow cytometry.

Dot Blot Assay

DNA was diluted to 100ng/μl and a dilution series was performed, then 1μl was spotted on a 0.45 μm pore size positively charged nylon membrane The membrane was air dried completely on a paper towel for 10 min at room temperature, followed by baking in a vacuum oven 80°C for 2 h. The membrane was blocked in 5% milk/TBS/0.1%Tween-20 for 1h, followed by incubation with 5hmC or 5mC antibodies in TBST/0.1% BSA overnight at 4°C overnight. Then they were treated with horseradish peroxidase-conjugated rabbit or mouse IgG (Santa Cruz) (1:10,000) for 1 h, enhanced with a SuperSignal® West Pico Chemiluminescent Substrate (Pierce, Rockford, IL), and exposed on BIOMAX MR films (Kodak, Rochester, NY).

Microarray

Total RNAs were extracted from control and *Cbs*$^{-/-}$ CD4$^+$ T cells with an RNeasy kit (Qiagen). Microarray assays were performed at the Genome Center of Children's Hospital, Los Angeles, using Mouse Gene 1.0 ST arrays (Affymetrix). The global gene expression difference was analyzed by Partek Genomics Suite and Ingenuity Pathway Analysis (IPA) software. Global gene expression profiles rank ordered by relative fold-change values were analyzed using Gene Set Enrichment Analysis software (Broad Institute, MIT).

Statistical analysis

Significance was determined by independent two–tailed Student's t–tests or one-way analysis of variance (ANOVA) using SPSS 18.0 software. Kaplan–Meier survival curves were constructed and analyzed by a log-rank test. At least four mice were randomly assigned to each group. Exact number of mice used in each group was indicated in the figure legends. Data were assessed for normal distribution and similar variance between groups prior to further statistic analysis. *P*-values less than 0.05 were considered significant.

Supplementary Material

Refer to Web version on PubMed Central for supplementary material.

Acknowledgments

This work was supported by grants from the National Institute of Dental and Craniofacial Research, National Institutes of Health, Department of Health and Human Services (R01DE017449 and R01DE019932 to S.S.), the Ministry of Science and Technology, China (2010DFB32980 to Y.Z.), and the Intramural Research Program of NIDCR, NIH (for W.J.C.).

Author Manuscript Author Manuscript Author Manuscript Author Manuscript

References

Chen W, Jin W, Hardegen N, Lei KJ, Li L, Marinos N, McGrady G, Wahl SM. Conversion of peripheral $CD4^+CD25^-$ naive T cells to $CD4^+CD25^+$ regulatory T cells by TGF-beta induction of transcription factor Foxp3. J Exp Med. 2003; 198:1875–1886. [PubMed: 14676299]

Costa Y, Ding J, Theunissen TW, Faiola F, Hore TA, Shliaha PV, Fidalgo M, Saunders A, Lawrence M, Dietmann S, et al. NANOG-dependent function of TET1 and TET2 in establishment of pluripotency. Nature. 2013; 495:370–374. [PubMed: 23395962]

Feng Y, Arvey A, Chinen T, van der Veeken J, Gasteiger G, Rudensky AY. Control of the Inheritance of Regulatory T Cell Identity by a cis Element in the Foxp3 Locus. Cell. 2014; 158:749–763. [PubMed: 25126783]

Fiorucci S, Orlandi S, Mencarelli A, Caliendo G, Santagada V, Distrutti E, Santucci L, Cirino G, Wallace JL. Enhanced activity of a hydrogen sulphide-releasing derivative of mesalamine (ATB-429) in a mouse model of colitis. British journal of pharmacology. 2007; 150:996–1002. [PubMed: 17339831]

Floess S, Freyer J, Siewert C, Baron U, Olek S, Polansky J, Schlawe K, Chang HD, Bopp T, Schmitt E, et al. Epigenetic control of the foxp3 locus in regulatory T cells. PLoS Biol. 2007; 5:e38. [PubMed: 17298177]

Grskovic M, Chaivorapol C, Gaspar-Maia A, Li H, Ramalho-Santos M. Systematic identification of cis-regulatory sequences active in mouse and human embryonic stem cells. PLoS genetics. 2007; 3:e145. [PubMed: 17784790]

Han Y, Zeng F, Tan G, Yang C, Tang H, Luo Y, Feng J, Xiong H, Guo Q. Hydrogen sulfide inhibits abnormal proliferation of lymphocytes via AKT/GSK3beta signal pathway in systemic lupus erythematosus patients. Cellular physiology and biochemistry : international journal of experimental cellular physiology, biochemistry, and pharmacology. 2013; 31:795–804.

Hori S, Nomura T, Sakaguchi S. Control of regulatory T cell development by the transcription factor Foxp3. Science. 2003; 299:1057–1061. [PubMed: 12522256]

Ichiyama K, Chen T, Wang X, Yan X, Kim BS, Tanaka S, Ndiaye-Lobry D, Deng Y, Zou Y, Zheng P, et al. The methylcytosine dioxygenase Tet2 promotes DNA demethylation and activation of cytokine gene expression in T cells. Immunity. 2015; 42:613–626. [PubMed: 25862091]

Kallin EM, Rodriguez-Ubreva J, Christensen J, Cimmino L, Aifantis I, Helin K, Ballestar E, Graf T. Tet2 facilitates the derepression of myeloid target genes during CEBPalpha-induced transdifferentiation of pre-B cells. Mol Cell. 2012; 48:266–276. [PubMed: 22981865]

Kelly PJ, Furie KL, Kistler JP, Barron M, Picard EH, Mandell R, Shih VE. Stroke in young patients with hyperhomocysteinemia due to cystathionine beta-synthase deficiency. Neurology. 2003; 60:275–279. [PubMed: 12552044]

Kim HP, Leonard WJ. CREB/ATF-dependent T cell receptor-induced FoxP3 gene expression: a role for DNA methylation. J Exp Med. 2007; 204:1543–1551. [PubMed: 17591856]

Koh KP, Yabuuchi A, Rao S, Huang Y, Cunniff K, Nardone J, Laiho A, Tahiliani M, Sommer CA, Mostoslavsky G, et al. Tet1 and Tet2 regulate 5-hydroxymethylcytosine production and cell lineage specification in mouse embryonic stem cells. Cell Stem Cell. 2011; 8:200–213. [PubMed: 21295276]

Kohli RM, Zhang Y. TET enzymes, TDG and the dynamics of DNA demethylation. Nature. 2013; 502:472–479. [PubMed: 24153300]

Konkel JE, Jin W, Abbatiello B, Grainger JR, Chen W. Thymocyte apoptosis drives the intrathymic generation of regulatory T cells. Proc Natl Acad Sci U S A. 2014; 111:E465–473. [PubMed: 24474796]

Kosower NS, Kosower EM, Wertheim B, Correa WS. Diamide, a new reagent for the intracellular oxidation of glutathione to the disulfide. Biochem Biophys Res Commun. 1969; 37:593–596. [PubMed: 5353890]

Kriaucionis S, Heintz N. The nuclear DNA base 5-hydroxymethylcytosine is present in Purkinje neurons and the brain. Science. 2009; 324:929–930. [PubMed: 19372393]

Author Manuscript Author Manuscript Author Manuscript Author Manuscript

Li L, Bhatia M, Zhu YZ, Zhu YC, Ramnath RD, Wang ZJ, Anuar FB, Whiteman M, Salto-Tellez M, Moore PK. Hydrogen sulfide is a novel mediator of lipopolysaccharide-induced inflammation in the mouse. FASEB J. 2005; 19:1196–1198. [PubMed: 15863703]

Li X, Liang Y, LeBlanc M, Benner C, Zheng Y. Function of a Foxp3 cis-element in protecting regulatory T cell identity. Cell. 2014; 158:734–748. [PubMed: 25126782]

Liu Y, Yang R, Liu X, Zhou Y, Qu C, Kikuiri T, Wang S, Zandi E, Du J, Ambudkar IS, et al. Hydrogen Sulfide Maintains Mesenchymal Stem Cell Function and Bone Homeostasis via Regulation of Ca Channel Sulfhydration. Cell Stem Cell. 2014

Mustafa AK, Gadalla MM, Sen N, Kim S, Mu W, Gazi SK, Barrow RK, Yang G, Wang R, Snyder SH. H2S signals through protein S-sulfhydration. Sci Signal. 2009; 2:ra72. [PubMed: 19903941]

Nair VS, Oh KI. Down-regulation of Tet2 prevents TSDR demethylation in IL2 deficient regulatory T cells. Biochemical and biophysical research communications. 2014; 450:918–924. [PubMed: 24984151]

Nardini M, Gnesutta N, Donati G, Gatta R, Forni C, Fossati A, Vonrhein C, Moras D, Romier C, Bolognesi M, et al. Sequence-specific transcription factor NF-Y displays histone-like DNA binding and H2B-like ubiquitination. Cell. 2013; 152:132–143. [PubMed: 23332751]

Ogawa C, Tone Y, Tsuda M, Peter C, Waldmann H, Tone M. TGF-beta-mediated Foxp3 gene expression is cooperatively regulated by Stat5, Creb, and AP-1 through CNS2. J Immunol. 2014; 192:475–483. [PubMed: 24298014]

Ohkura N, Hamaguchi M, Morikawa H, Sugimura K, Tanaka A, Ito Y, Osaki M, Tanaka Y, Yamashita R, Nakano N, et al. T cell receptor stimulation-induced epigenetic changes and Foxp3 expression are independent and complementary events required for Treg cell development. Immunity. 2012; 37:785–799. [PubMed: 23123060]

Paul BD, Snyder SH. H(2)S signalling through protein sulfhydration and beyond. Nat Rev Mol Cell Biol. 2012; 13:499–507. [PubMed: 22781905]

Peng YJ, Makarenko VV, Nanduri J, Vasavda C, Raghuraman G, Yuan G, Gadalla MM, Kumar GK, Snyder SH, Prabhakar NR. Inherent variations in CO-H2S-mediated carotid body O2 sensing mediate hypertension and pulmonary edema. Proc Natl Acad Sci U S A. 2014; 111:1174–1179. [PubMed: 24395806]

Sen N, Paul BD, Gadalla MM, Mustafa AK, Sen T, Xu R, Kim S, Snyder SH. Hydrogen sulfide-linked sulfhydration of NF-kappaB mediates its antiapoptotic actions. Mol Cell. 2012; 45:13–24. [PubMed: 22244329]

Shevach EM. Regulatory T cells in autoimmmunity*. Annu Rev Immunol. 2000; 18:423–449. [PubMed: 10837065]

Song SJ, Poliseno L, Song MS, Ala U, Webster K, Ng C, Beringer G, Brikbak NJ, Yuan X, Cantley LC, et al. MicroRNA-antagonism regulates breast cancer stemness and metastasis via TET-family-dependent chromatin remodeling. Cell. 2013; 154:311–324. [PubMed: 23830207]

Szabo C, Coletta C, Chao C, Modis K, Szczesny B, Papapetropoulos A, Hellmich MR. Tumor-derived hydrogen sulfide, produced by cystathionine-beta-synthase, stimulates bioenergetics, cell proliferation, and angiogenesis in colon cancer. Proc Natl Acad Sci U S A. 2013; 110:12474–12479. [PubMed: 23836652]

Tahiliani M, Koh KP, Shen Y, Pastor WA, Bandukwala H, Brudno Y, Agarwal S, Iyer LM, Liu DR, Aravind L, et al. Conversion of 5-methylcytosine to 5-hydroxymethylcytosine in mammalian DNA by MLL partner TET1. Science. 2009; 324:930–935. [PubMed: 19372391]

Toker A, Engelbert D, Garg G, Polansky JK, Floess S, Miyao T, Baron U, Duber S, Geffers R, Giehr P, et al. Active demethylation of the Foxp3 locus leads to the generation of stable regulatory T cells within the thymus. J Immunol. 2013; 190:3180–3188. [PubMed: 23420886]

Tsagaratou A, Aijo T, Lio CW, Yue X, Huang Y, Jacobsen SE, Lahdesmaki H, Rao A. Dissecting the dynamic changes of 5-hydroxymethylcytosine in T-cell development and differentiation. Proc Natl Acad Sci U S A. 2014; 111:E3306–3315. [PubMed: 25071199]

Vignali DA, Collison LW, Workman CJ. How regulatory T cells work. Nat Rev Immunol. 2008; 8:523–532. [PubMed: 18566595]

Author Manuscript Author Manuscript Author Manuscript Author Manuscript

Wang L, Liu Y, Han R, Beier UH, Thomas RM, Wells AD, Hancock WW. Mbd2 promotes foxp3 demethylation and T-regulatory-cell function. Mol Cell Biol. 2013; 33:4106–4115. [PubMed: 23979593]

Wang R. Two's company, three's a crowd: can H_2S be the third endogenous gaseous transmitter? FASEB J. 2002; 16:1792–1798. [PubMed: 12409322]

Watanabe M, Osada J, Aratani Y, Kluckman K, Reddick R, Malinow MR, Maeda N. Mice deficient in cystathionine beta-synthase: animal models for mild and severe homocyst(e)inemia. Proc Natl Acad Sci U S A. 1995; 92:1585–1589. [PubMed: 7878023]

Williams K, Christensen J, Pedersen MT, Johansen JV, Cloos PA, Rappsilber J, Helin K. TET1 and hydroxymethylcytosine in transcription and DNA methylation fidelity. Nature. 2011; 473:343–348. [PubMed: 21490601]

Wu H, Zhang Y. Reversing DNA methylation: mechanisms, genomics, and biological functions. Cell. 2014; 156:45–68. [PubMed: 24439369]

Xu Y, Wu F, Tan L, Kong L, Xiong L, Deng J, Barbera AJ, Zheng L, Zhang H, Huang S, et al. Genome-wide regulation of 5hmC, 5mC, and gene expression by Tet1 hydroxylase in mouse embryonic stem cells. Mol Cell. 2011; 42:451–464. [PubMed: 21514197]

Yamanaka T, Tosaki A, Kurosawa M, Matsumoto G, Koike M, Uchiyama Y, Maity SN, Shimogori T, Hattori N, Nukina N. NF-Y inactivation causes atypical neurodegeneration characterized by ubiquitin and p62 accumulation and endoplasmic reticulum disorganization. Nature communications. 2014; 5:3354.

Zhang G, Wang P, Yang G, Cao Q, Wang R. The inhibitory role of hydrogen sulfide in airway hyperresponsiveness and inflammation in a mouse model of asthma. Am J Pathol. 2013; 182:1188–1195. [PubMed: 23395089]

Zhang J, Sio SW, Moochhala S, Bhatia M. Role of hydrogen sulfide in severe burn injury-induced inflammation in mice. Molecular medicine. 2010; 16:417–424. [PubMed: 20440442]

Zheng Y, Josefowicz S, Chaudhry A, Peng XP, Forbush K, Rudensky AY. Role of conserved non-coding DNA elements in the Foxp3 gene in regulatory T-cell fate. Nature. 2010; 463:808–812. [PubMed: 20072126]

Zheng Y, Josefowicz SZ, Kas A, Chu TT, Gavin MA, Rudensky AY. Genome-wide analysis of Foxp3 target genes in developing and mature regulatory T cells. Nature. 2007; 445:936–940. [PubMed: 17237761]

Author Manuscript Author Manuscript Author Manuscript Author Manuscript

Highlights

- H_2S is required for Treg cell differentiation and immune homeostasis.
- H_2S deficiency results in decreased Tet1 and Tet2 expression in T cells.
- Synergism between Tet and TGF-β and IL-2 signaling regulate Treg cell function.
- Depletion of *Tet1* and *Tet2* leads to impairment of Treg cell differentiation.

Author Manuscript Author Manuscript Author Manuscript Author Manuscript

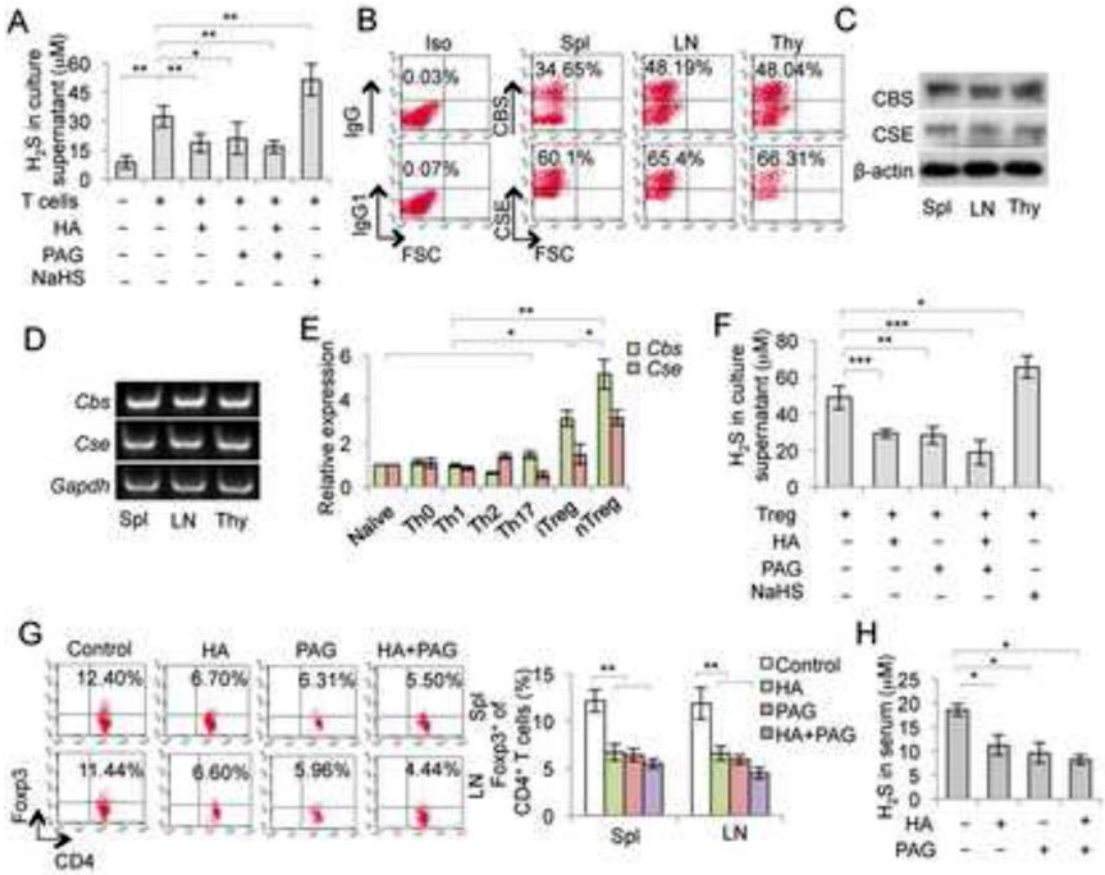

Figure 1. H_2S-deficient T cells show impaired Treg cell differentiation

(**A**) H_2S production in $CD4^+$ T cell culture supernatant after treatment with CBS inhibitor HA, CSE inhibitor PAG, HA and PAG combination or H_2S donor NaHS. (**B–D**) CBS and CSE expression in $CD4^+$ T cells from mouse spleen (Spl), lymph nodes (LN), and thymus (Thy) are analyzed by flow cytometry (**B**), Western blot (**C**) and PCR (**D**). (**E**) *Cbs* and *Cse* expression in different T cells subsets including Naïve, Th0, Th1, Th2, Th17 and Treg cells (iTreg and nTreg) are shown, as assessed by qPCR analysis. (**F**) H_2S production in Treg cell culture supernatant in indicated groups. (**G**) The frequency of Treg cells in spleen and lymph nodes after 5 weeks of HA (n=4), PAG (n=4) or HA and PAG combined treatment (n=4) in mice are shown, as assessed by flow cytometry. (**H**) The mouse serum concentrations after HA, PAG or HA and PAG combined injection are shown. Statistical significance is determined with one-way ANOVA (A, F–H). * P<0.05, ** P< 0.01, *** P<0.001, (mean ±SD) Results are from three repeated experiments.

Author Manuscript Author Manuscript Author Manuscript Author Manuscript

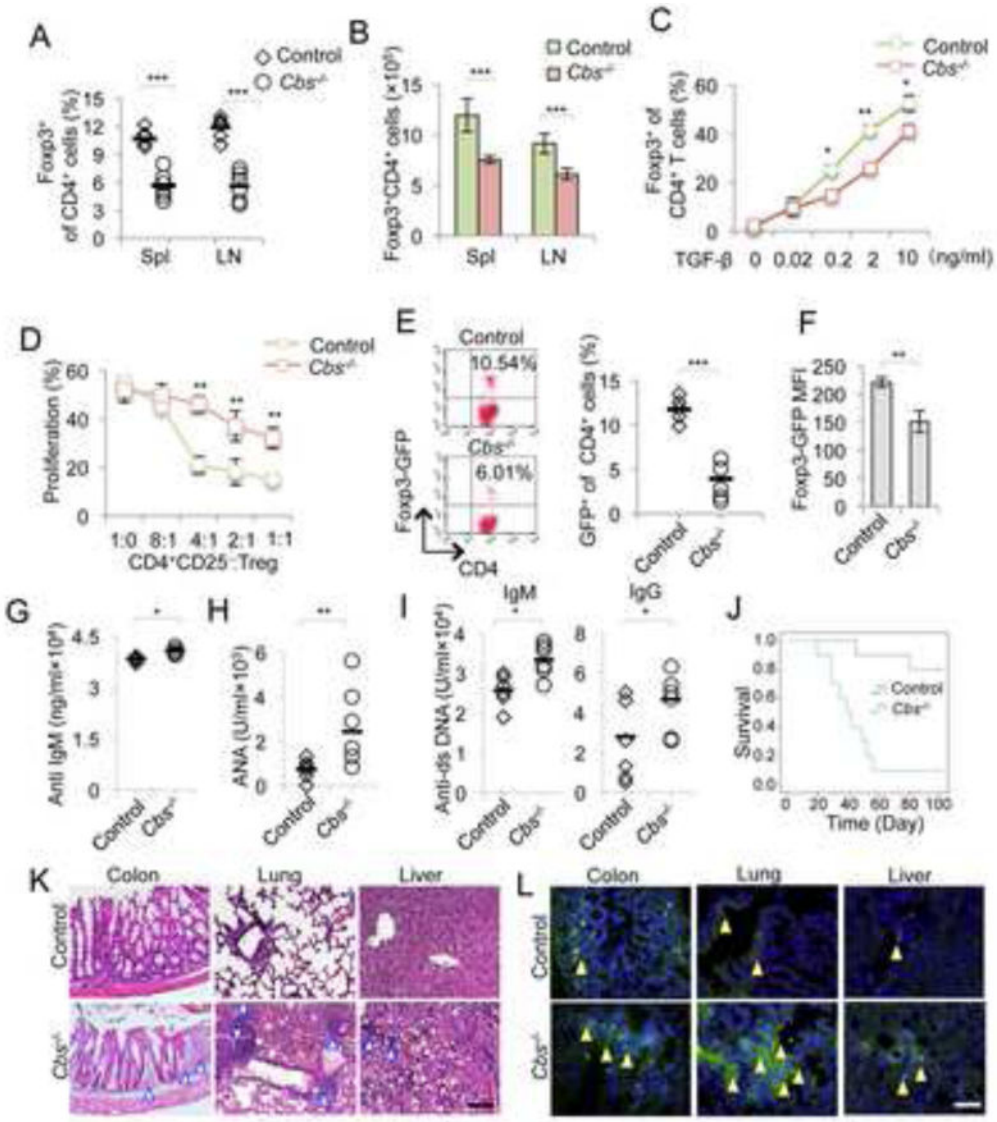

Figure 2. H_2S-deficient mice show Treg cell impairment and autoimmune diseases

(**A**) Treg cell frequency in control and *Cbs*$^{-/-}$ mice spleen (Spl) and lymph nodes (LN) are assessed by flow cytometry. (**B**) The total numbers of Foxp3^{+} Treg cells in control and *Cbs*$^{-/-}$ mice. (**C**) Control and *Cbs*$^{-/-}$ naïve T cells *in vitro* differentiation induced by 2ng/ml IL-2 and a range of doses of TGF-β are shown. (**D**) Suppressive assay of Treg cells from control and *Cbs*$^{-/-}$ mice. (**E, F**) Treg cells frequency and Foxp3 expression in spleen of *Foxp3*^{GFP} and *Cbs*$^{-/-}$ *Foxp3*^{GFP} mice are assessed by flow cytometry. (**G–I**) Auto-reactive antibodies including anti-autoactive antibody IgM (**G**), anti-nuclear antibody (ANA) (**H**), and dsDNA antibodies IgM and IgG (**I**) in control and *Cbs*$^{-/-}$ mouse serum are measured by ELISA (n=6). (**J**) Kaplan–Meier survival curves of *Cbs*$^{-/-}$ mice (n=10) and control littermates (n=10). (**K**) Histological structures of the mouse colon, lung and liver at 5–6 weeks are shown, as assessed by haematoxylin and eosin (HE) staining. Inflammation cells infiltration is indicated (blue triangle). (**L**) CD3^{+} lymphocyte infiltration (yellow triangle) in colon, lung and liver is analyzed by immunofluorescence staining. Statistical significance is

Author Manuscript Author Manuscript Author Manuscript Author Manuscript

determined by two–tailed Student's t–tests (A–I), Kaplan–Meier survival curves are constructed and analyzed by a log-rank test (J, $P<0.001$) * $P<0.05$, ** $P< 0.01$, *** $P< 0.001$, (mean±SD). Scale bars: HE, 100 μm. Immunofluorescence staining, 50 μm. Results are from three repeated experiments.

Author Manuscript Author Manuscript Author Manuscript Author Manuscript

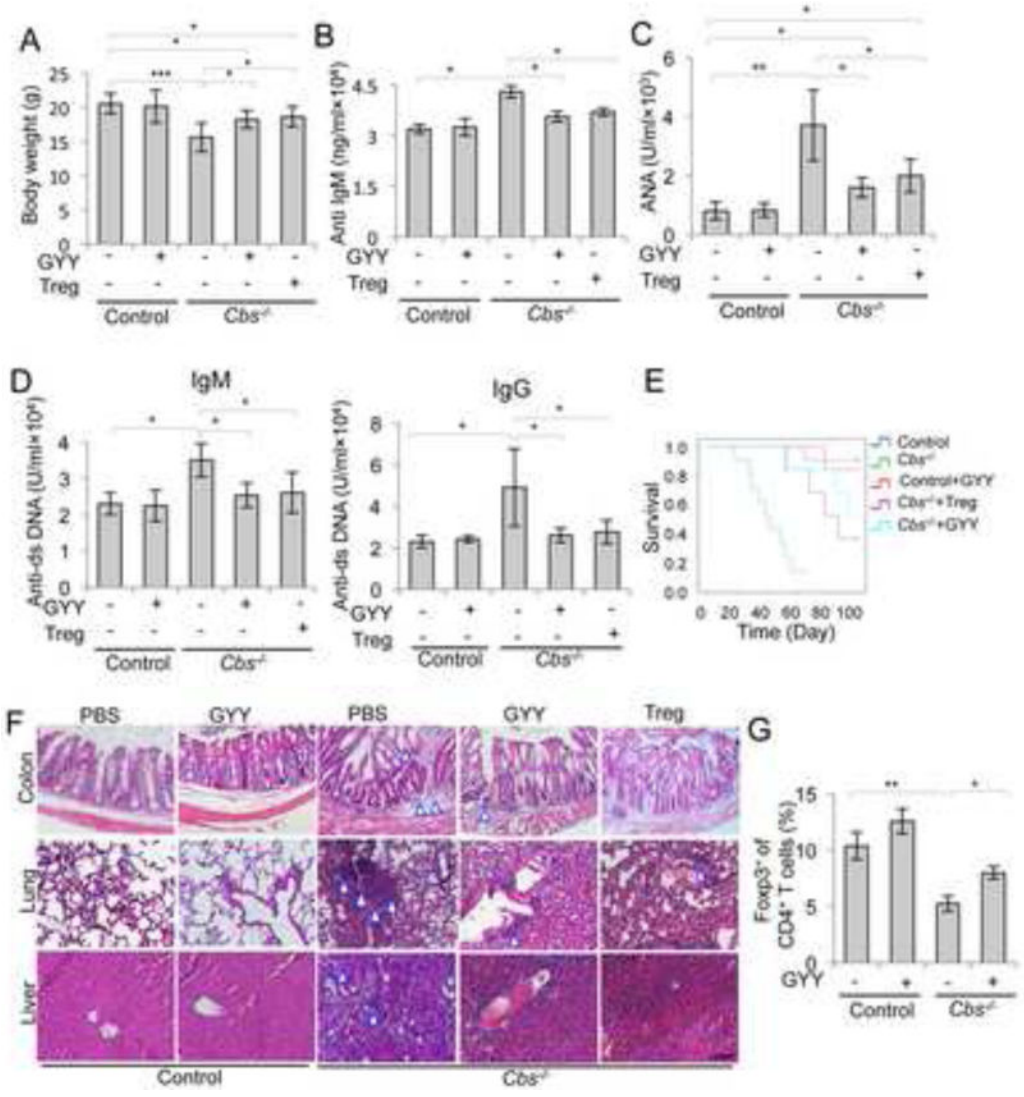

Figure 3. H_2S is required for maintenance of immune homeostasis *via* regulating Treg cells

(**A–E**) Mouse body weight (**A**), autoreactive antibodies, including anti-autoactive antibody IgM (**B**), ANA (**C**) and anti-dsDNA antibodies IgM and IgG (**D**), and mouse survival curves (**E**) with or without H_2S donor GYY4137 injection (n=6) or Treg cell infusion (n=6) are shown. (**F**) HE staining shows the histological structure of colon, lung and liver in indicated groups. Inflammatory cells infiltration is indicated by blue triangle. (**G**) Proportion of $Foxp3^+$ Treg cells after GYY4137 injection in control and $Cbs^{-/-}$ mice. Statistical significance is determined by one-way ANOVA (A–D, G), Kaplan–Meier survival curves are constructed and analyzed by a log-rank test (E, $Cbs^{-/-}$ vs control: $P<0.001$; $Cbs^{-/-}$+Treg vs $Cbs^{-/-}$: $P<0.05$; $Cbs^{-/-}$+Treg vs control: $P<0.05$; $Cbs^{-/-}$+GYY vs $Cbs^{-/-}$: $P<0.01$; $Cbs^{-/-}$+GYY vs control: $P<0.05$) * $P<0.05$, ** $P< 0.01$, *** $P< 0.001$. * (mean±SD). Scale bar: 100μm. Results are from three repeated experiments.

Author Manuscript Author Manuscript Author Manuscript Author Manuscript

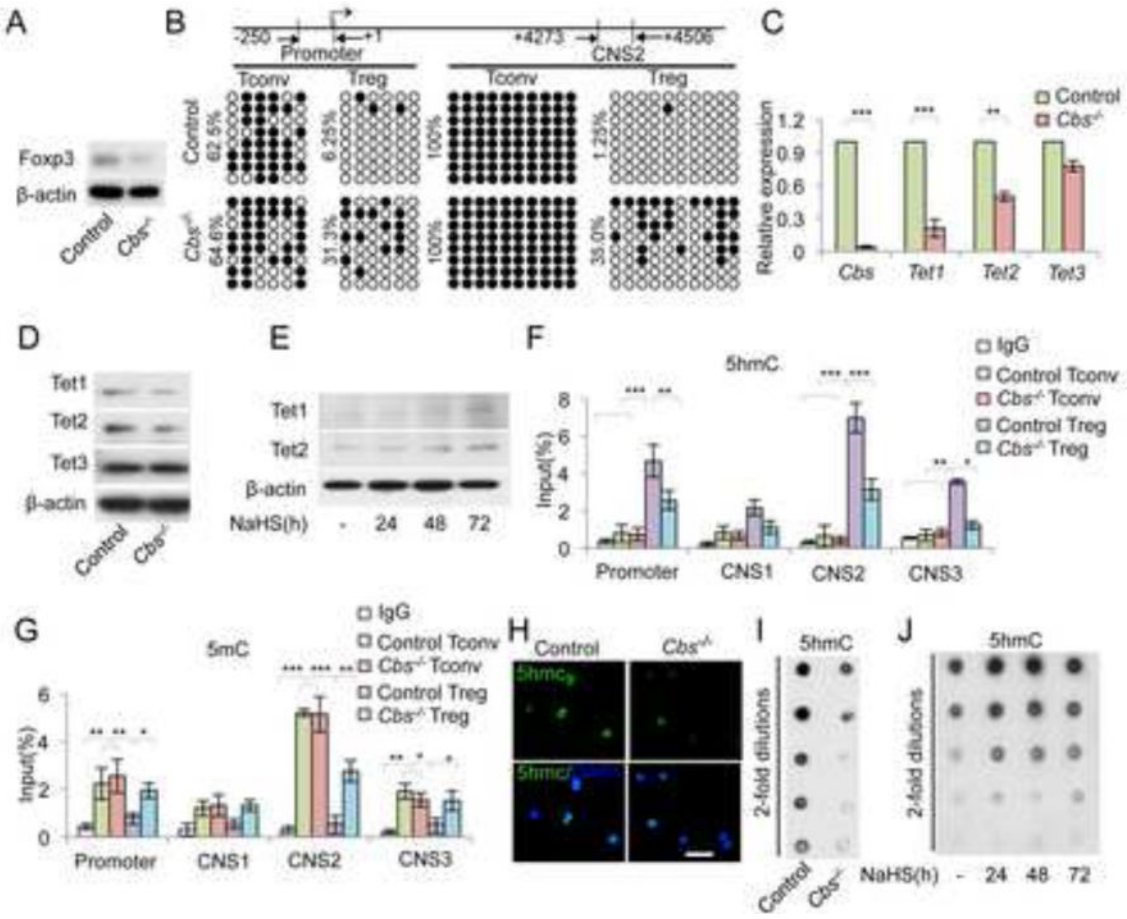

Figure 4. H_2S targets Tet1 and Tet2 to convert 5mC to 5hmC

(**A**) Foxp3 expression in control and *Cbs*$^{-/-}$ Treg cells are shown. (**B**) The methylation status in promoter and CNS2 region of *Fopx3* in control and *Cbs*$^{-/-}$ CD4^{+}Foxp3^{-} Tconv cells and Treg cells analyzed by OxBS-sequencing. Each row of dots represents CpG sites in *Foxp3* promoter and CNS2 region; each dot represents a single CpG. Empty dots indicate unmethylated CpGs; black dots indicate methylated CpGs. (**C, D**) The expression of Tet1, Tet2 and Tet3 in CD4^{+} T cells from control and *Cbs*$^{-/-}$ mice are assessed by Western blot and qPCR. (**E**) Tet1 and Tet2 expression in CD4^{+} T cells treated with H_2S donor NaHS are shown. (**F, G**) Enrichments of 5hmC and 5mC in *Foxp3* promoter and CNS1-3 regions are assessed by hMeDIP-qPCR and MeDIP-qPCR analysis, respectively. IgG was used as a control. (**H, I**) 5hmC expression in CD4^{+} T cells are assessed by immunofluorescence staining and dot blot assay analysis. (**J**) Global 5hmC expression in CD4^{+} T cells treated by H_2S donor NaHS are shown. Statistical significance is determined by two–tailed Student's t–tests (C) or one-way ANOVA (F, G). *P<0.05, **P< 0.01, *** P< 0.001. (mean±SD) Scale bar: 25 μm. Results are from three repeated experiments.

Author Manuscript Author Manuscript Author Manuscript Author Manuscript

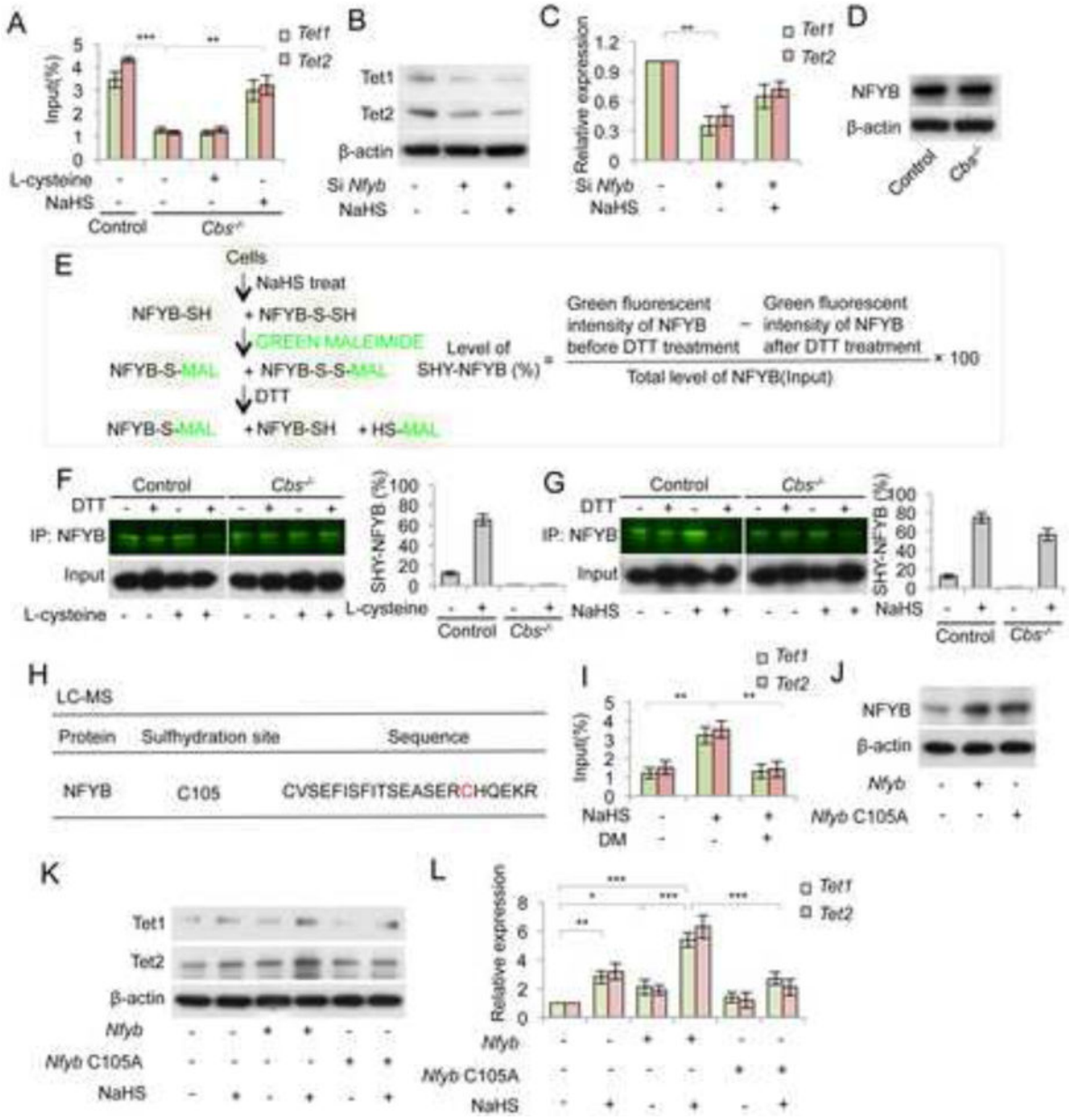

Figure 5. H_2S regulates Tet1 and Tet2 expression *via* sulfhydration of NFYB

(**A**) NFYB enrichments in the promoters of *Tet1* and *Tet2* are analyzed by ChIP-qPCR. (**B, C**) The expression of Tet1 and Tet2 in $CD4^+$ T cells after indicated treatment are assessed by Western blot and qPCR. (**D**) Western blot demonstrating NFYB expression in control and $Cbs^{-/-}$ T cells. (**E**) Schematic diagram for detection of NFYB sulfhydration with green maleimide. (**F, G**) The green signal of NFYB protein after indicated treatment in control and $Cbs^{-/-}$ T cells. (**H**) LC-MS analysis of sulfhydration in NFYB protein Cys105 after NaHS (1mM) treatment. (**I**) ChIP-qPCR analyzes NFYB enrichment in the promoters of *Tet1* and *Tet2* in $Cbs^{-/-}$ T cells in indicated treatments. (**J**) NFYB expression in $CD4^+$ T cells without or with *Nfyb* or *Nfyb* C105A plasmids transfection are analyzed by Western blot. (**K, L**) The expression of Tet1 and Tet2 in $CD4^+$ T cells after indicated treatments are assessed by

Author Manuscript Author Manuscript Author Manuscript Author Manuscript

Western blot and qPCR. Statistical significance is by one-way ANOVA (A, C, I, L). **P<0.05, **P<0.01, *** P<0.001. (mean±SD). Results are from three repeated experiments.

Author Manuscript Author Manuscript Author Manuscript Author Manuscript

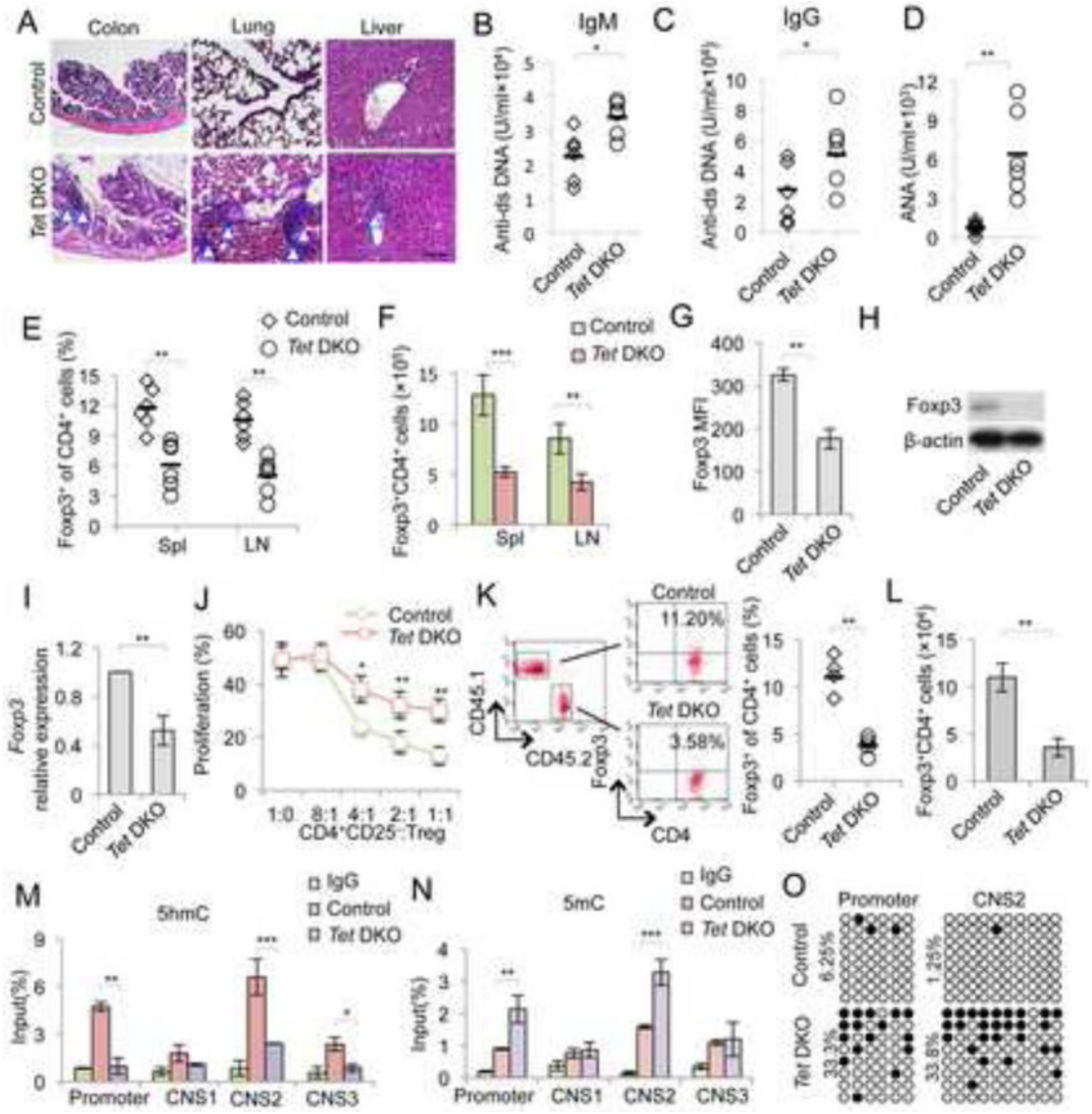

Figure 6. Tet1 and Tet2 are required for Treg cell differentiation and function

(**A**) HE staining show inflammatory cell infiltration (blue triangle) in the colon, lung and liver of *Tet1*$^{-/-}$; *Cd4*^{Cre}; *Tet2*$^{fl/fl}$ (*Tet* DKO) mice, *Tet2*$^{fl/fl}$ mice are used as control. (**B–D**) The anti-dsDNA antibodies IgM (**B**) and IgG (**C**), and anti ANA (**D**) are measured by ELISA in control and *Tet* DKO mouse serum. (**E**) Treg cell frequencies in the spleen (Spl) and lymph nodes (LN) from control and *Tet* DKO mice are shown. (**F**) The total numbers of Foxp3^{+} Treg cells are shown. (**G–I**) Foxp3 expression in control and *Tet* DKO Treg cells are assessed by flow cytometry (**G**), Western blot (**H**) and qPCR (**I**). (**J**) Suppressive capacities of *Tet* DKO Treg cells and control ones are shown. (**K–L**) WT control (CD45.1) and *Tet* DKO (CD45.2) bone marrow cells co-transferred into sublethally irradiated WT recipient mice (n=4) for 6 weeks to generate mixed bone marrow chimeric mice. Representative flow cytometry plots of splenic CD45.1 and CD45.2 cells are shown. Percentages (**K**) and numbers (**L**) of CD4^{+}Foxp3^{+} Treg cells are shown. (**M, N**) Enrichments of 5hmC (**M**) and 5mC (**N**) within *Foxp3* promoter and CNS1-3 regions in control and *Tet* DKO Treg cells are

Author Manuscript Author Manuscript Author Manuscript Author Manuscript

assessed by hMeDIP-qPCR and MeDIP-qPCR analysis, respectively. IgG is used as a control. (**O**) OxBS-sequencing analysis show the promoter and CNS2 region methylation status of *Foxp3* in Treg cells. Statistical significance is determined by two–tailed Student's t–tests (B–G, I–L) and one-way ANOVA (M, N). **P*<0.05, ***P*<0.01, *** *P*<0.001. (mean ±SD) Scale bar: 100 μm. Results are from three repeated experiments.

Author Manuscript Author Manuscript Author Manuscript Author Manuscript

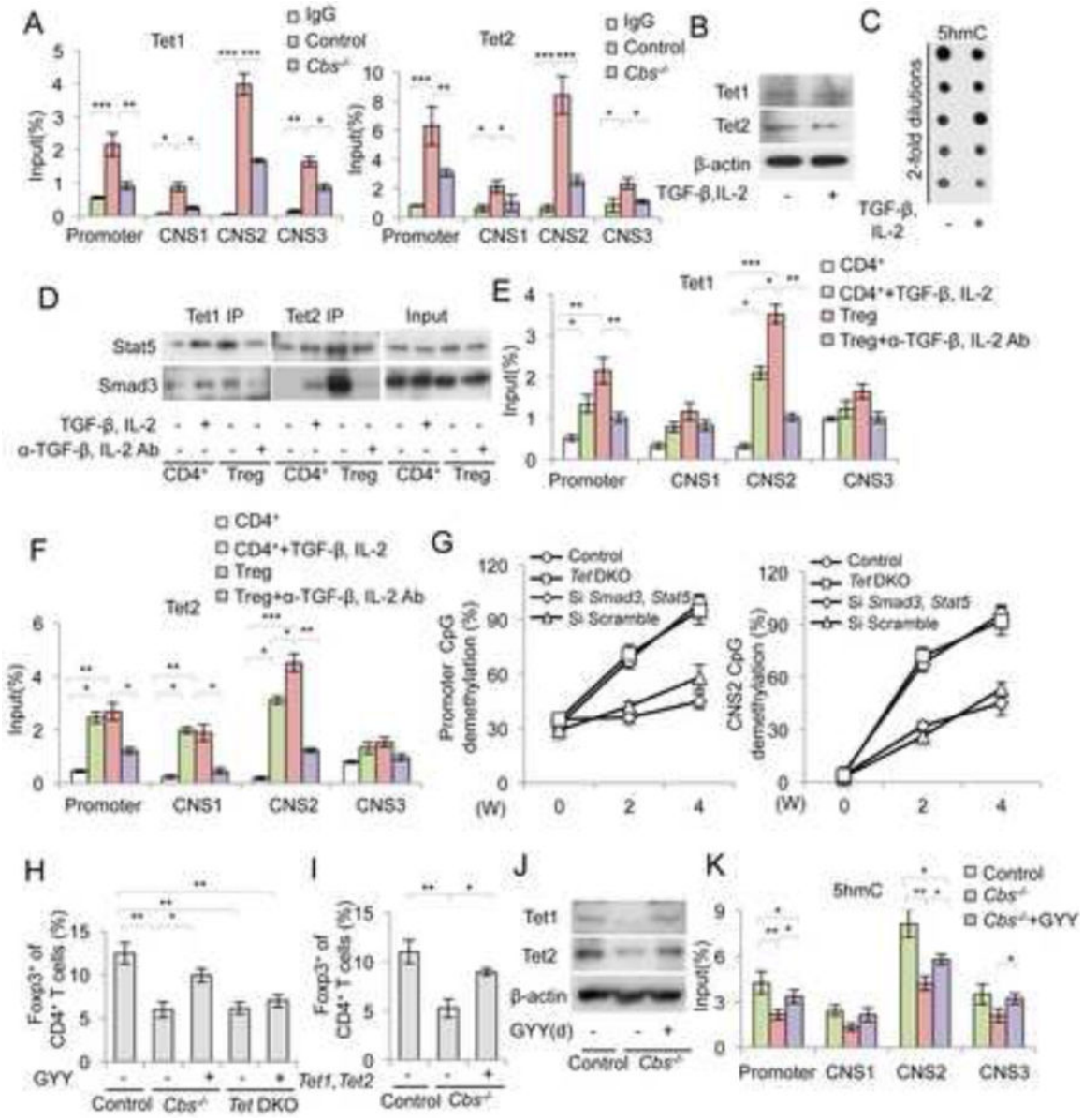

Figure 7. Activated Smad3 and Stat5 recruit Tet1 and Tet2 binding to *Foxp3* locus

(**A**) ChIP-qPCR analyzes Tet1 and Tet2 binding in the promoter and CNS regions of *Foxp3* in Treg cells. IgG is used as control. (**B, C**) Tet1 and Tet2 expression (**B**) and global 5hmC levels (**C**) in $CD4^+$ T cells treated with TGF-β and IL-2 are assessed by Western blot and dot blot assay, respectively. (**D**) Tet1 and Tet2 interaction with Smad3 and Stat5 in $CD4^+$ T cells and Treg cells by indicated treatments are assessed by protein complex immunoprecipitation (Co-IP) assay. (**E, F**) Tet1 and Tet2 binding activity to the promoter and CNS1-3 regions of *Foxp3* in $CD4^+$ T cells and Treg cells are analyzed by ChIP-qPCR. (**G**) $CD4^+CD25^-Foxp3^{GFP-}$ T cells from control and *Tet* DKO mice are transferred into *Rag1*$^{-/-}$ mice (n=4). The generated $CD4^+Foxp3^{GFP+}$ cells are isolated for methylation analysis and show the demethylation ratios of *Foxp3* promoter and CNS2 in indicated groups. (**H**) Treg cell frequencies in *Cbs*$^{-/-}$ mice (n=4) and *Tet* DKO mice (n=4) with or without GYY4137

Author Manuscript Author Manuscript Author Manuscript Author Manuscript

(GYY) injection (n=4) are shown, as assessed by flow cytometry. (**I**) Treg cell frequency in *Rag1*$^{-/-}$ mice (n=4) after transferring control, *CBS*$^{-/-}$, or *Tet1* and *Tet2* overexpressed *CBS*$^{-/-}$ CD4^{+} naïve T cells, as assessed by flow cytometry. (**J**) Tet1 and Tet2 expression in CD4^{+} T cells after GYY4137 injection in *Cbs*$^{-/-}$ mice are shown. (**K**) 5hmC enrichment within the promoter and CNS1-3 regions of *Foxp3* in Treg cells with or without GYY4137 injection in *Cbs*$^{-/-}$ mice are analyzed by hMeDIP-qPCR. Statistical significance is determined by one-way ANOVA (A, E, F, H, I, K). * P<0.05, ** P< 0.01, *** P< 0.001. (mean±SD). Results are from three repeated experiments.